ARTICLE

Physiologically based pharmacokinetic–pharmacodynamic modeling for prediction of vonoprazan pharmacokinetics and its inhibition on gastric acid secretion following intravenous/oral administration to rats, dogs and humans

Wei-min Kong[1], Bin-bin Sun[1], Zhong-jian Wang[1], Xiao-ke Zheng[1], Kai-jing Zhao[1], Yang Chen[1], Jia-xin Zhang[1], Pei-hua Liu[1], Liang Zhu[1], Ru-jun Xu[1], Ping Li[1], Li Liu[1] and Xiao-dong Liu[1]

Vonoprazan is characterized as having a long-lasting antisecretory effect on gastric acid. In this study we developed a physiologically based pharmacokinetic (PBPK)-pharmacodynamic (PD) model linking to stomach to simultaneously predict vonoprazan pharmacokinetics and its antisecretory effects following administration to rats, dogs, and humans based on in vitro parameters. The vonoprazan disposition in the stomach was illustrated using a limited-membrane model. In vitro metabolic and transport parameters were derived from hepatic microsomes and Caco-2 cells, respectively. We found the most predicted plasma concentrations and pharmacokinetic parameters of vonoprazan in rats, dogs and humans were within twofold errors of the observed data. Free vonoprazan concentrations ($f_u \times C_2$) in the stomach were simulated and linked to the antisecretory effects of the drug (I) (increases in pH or acid output) using the fomula $dI/dt = k \times f_u \times C_2 \times (I_{max} - I) - k_d \times I$. The vonoprazan dissociation rate constant k_d (0.00246 min^{-1}) and inhibition index K_I (35 nM) for H$^+$/K$^+$-ATPase were obtained from literatures. The vonoprazan-H$^+$/K$^+$-ATPase binding rate constant k was 0.07028 min$^{-1}\cdot\mu$M^{-1} using ratio of k_d to K_I. The predicted antisecretory effects were consistent with the observations following intravenous administration to rats (0.7 and 1.0 mg/kg), oral administration to dogs (0.3 and 1.0 mg/kg) and oral single dose or multidose to humans (20, 30, and 40 mg). Simulations showed that vonoprazan concentrations in stomach were 1000-fold higher than those in the plasma at 24 h following administration to human. Vonoprazan pharmacokinetics and its antisecretory effects may be predicted from in vitro data using the PBPK-PD model of the stomach. These findings may highlight 24-h antisecretory effects of vonoprazan in humans following single-dose or the sustained inhibition throughout each 24-h dosing interval during multidose administration.

Keywords: vonoprazan; physiologically based pharmacokinetic–pharmacodynamic model; gastric acid secretion; pharmacokinetics; pharmacodynamics; potassium-competitive acid blocker

INTRODUCTION

Vonoprazan, first developed as its fumarate (TAK-438), is a potassium-competitive acid blocker, showing stronger and longer inhibition on H$^+$/K$^+$ ATPase [1–3] compared to traditional proton pump inhibitors (PPIs). Different from PPIs, vonoprazan is a basic amine (pKa = 9.06) [4], is metabolized mainly by CYP3A4 and might have less interpatient variability [5]. Vonoprazan has been approved for sale in Japan [6] at a common clinical dose of 20 mg [6–8]. In addition to CYP3A4, other enzymes such as CYP2B6, CYP2C19, CYP2D6, and a non-CYP enzyme SULT2A1 have also been reported to catalyze vonoprazan metabolism [9]. Clinical trials have shown that the efficacy of vonoprazan-based triple therapy (vonoprazan 20 mg, amoxicillin 750 mg, clarithromycin 200 or 400 mg) in *Helicobacter pylori* eradication is superior (eradication rates, 87.9% vs. 72.8%) [10] or at least noninferior to PPI-based triple therapies (eradication rates, 97.4% vs. 86.3%) [8]. The metabolism of vonoprazan has been widely studied [1, 9] and none of the metabolites has pharmacological activity [2]. In rats and dogs, the compound is almost completely metabolized [1]. Vonoprazan is mainly metabolized by oxidative deamination to 5-(2-fluorophenyl)-1-(pyridin-3-ylsulfonyl)-1H-pyrrole-3-carboxylic acid (M-I). M-I is further metabolized to 5-(2-fluorophenyl)-1H-pyrrole-3-carboxylic acid (M-II) by cleavage of the sulfonamide. The metabolites M-I and M-II conjugate with glucuronic acid to form M-I-G and M-II-G, respectively [1]. It has been reported that the summed exposure of M-I, M-II, M-I-G, and M-II-G in plasma following single oral administration of [^{14}C]TAK-438 to rats and dogs accounted for 76% and 68% of the total exposure, indicating that M-I was the main primary metabolite of vonoprazan [1]. M-I is also the primary metabolite of vonoprazan in humans, mainly catalyzed by cytochrome P450 3A4 [9].

[1]Center of Drug Metabolism and Pharmacokinetics, School of Pharmacy, China Pharmaceutical University, Nanjing 210009, China
Correspondence: Li Liu (liulee@yeah.net) or Xiao-dong Liu (xdliu@cpu.edu.cn)

Prediction of vonoprazan PK and PD using PBPK-PD model
WM Kong et al.

853

Several reports have demonstrated that the plasma exposure of M-I is the highest among the indicated metabolites [9, 11].

For a new candidate drug prior to its clinical phase, it is crucial and meaningful to gain a prediction of its pharmacokinetic profile in humans based on the limited information from in vitro and animal studies. Both whole body physiologically based pharmacokinetic (PBPK) models and interspecies allometric scaling are often used to accomplish the prediction. One advantage of PBPK model over interspecies allometric scaling is that the prediction may be accomplished from in vitro and in silico data. The PBPK model can also predict drug disposition in tissues to better explain the relationship between drug exposure in targeted tissue and its safety/efficacy. Vonoprazan shows its inhibitory effects (pharmacodynamic, PD) on gastric acid secretion via inhibiting H^+/K^+ ATPase. The stomach serves as its target organ, indicating that its antisecretory effects should be directly related to the vonoprazan concentration in the stomach rather than that in the plasma. The in vitro PD characteristics of vonoprazan have been widely investigated [4, 12, 13]. It is assumed that some intrinsic links may exist between the in vitro and in vivo PD characteristics of vonoprazan.

The aim of this study was to develop a whole-body PBPK-PD model of the stomach to monitor vonoprazan pharmacokinetics and its antisecretory effects on gastric acid following oral or intravenous administration to rats, dogs, and humans based on in vitro pharmacokinetic parameters (from hepatic microsomes and Caco-2 cells) and in vitro PD parameters from the literature [4, 13]. The pharmacokinetic behavior and antisecretory effects of vonoprazan were further predicted and verified by the observed data following intravenous or oral administration to rats, dogs and humans. These findings may highlight the 24-h suppression of gastric acid secretion in healthy male subjects following single-dose administration [5] or the sustained suppression of gastric acid secretion throughout each 24-h dosing interval during multidose administration [3, 14, 15], although no accumulation of vonoprazan occurred in plasma.

MATERIALS AND METHODS
Chemicals and reagents
Both vonoprazan acetate (purity 99.5%) and vonoprazan fumarate (purity 99.7%) and their metabolite M-I (purity 98.44%) were provided by Jiangsu Carefree Pharmaceutical Co. Ltd. Research Institute (Nanjing, China). The internal standard repaglinide (purity 99.7%) was purchased from National Institutes for Food and Drug Control (Beijing, China). Dog (male beagle dog, Lot. UKHU, mixed from 3 dogs) and human (male Mongolia human, Co. Ltd. SHQY, mixed from 11 individuals) hepatic microsomes were purchased from Research Institute of Liver Diseases (Shanghai, China). D-glucose-6-phosphate, glucose-6-phosphate dehydrogenase and β-$NADP^+$ were purchased from Sigma-Aldrich (St. Louis, Mo, USA). Other chemicals and reagents were of analytical grade or better.

Animals
Female adult Sprague Dawley rats (weighing 200–250 g) were obtained from Sino-British SIPPR/BK Lab Animal, Co. Ltd. (Shanghai, China) and beagles (7–10 kg) were obtained from Jambo Biological Technology Co. Ltd. (Shanghai China). All animals were housed in a normal 12-h light/dark cycle at constant temperature and humidity. All experiments were performed in accordance with institutional guidelines for the care and use of laboratory animals, which were approved by the Animal Ethics Committee of China Pharmaceutical University.

Pharmacokinetics in rats
Twenty-five rats were divided into five groups ($n = 5$), which were defined as intravenous low dose (base, 0.5 mg/kg), intravenous medium dose (base, 1 mg/kg), intravenous high dose of vonoprazan acetate (base, 2 mg/kg), oral dose (base, 2 mg/kg) of vonoprazan fumarate and intravenous multidose of vonoprazan acetate. For the single-dose conditions, the rats received intravenous administration of vonoprazan acetate or oral administration of vonoprazan fumarate. For the multidose condition, the rats received intravenous administration of vonoprazan acetate (base, 1 mg/kg) once a day for 7 days. Blood samples (approximately 0.15 mL) were collected in a heparin-treated tube via the postorbital venous plexus veins under light ether anesthesia at predose and 2, 5, 10, 20, 30, 45, 60, 90, 120, 180, and 240 min postdose.

The tissue distribution of vonoprazan in rats was also investigated. Another 15 rats were randomly divided into 3 groups of 5 rats each. The rats were sacrificed at 10, 60, and 180 min following intravenous administration of vonoprazan acetate (1 mg/kg, base). Blood, heart, liver, spleen, lungs, kidneys, stomach, intestines, brain, skin, fat, and muscle samples were quickly collected. Approximately, 0.2 g of the tissues were homogenized in 1.0 mL water.

Pharmacokinetics in dogs
Eight beagles (4 females and 4 males) were divided into A–D for 4 crossover designs with a 5-day wash out. Overnight, the dogs received a low dose of vonoprazan acetate (base, 0.15 mg/kg), a medium dose of vonoprazan acetate (base, 0.3 mg/kg), or a high dose of vonoprazan acetate intravenously (base, 0.6 mg/kg) or oral administration of vonoprazan fumarate (base, 0.6 mg/kg). Blood samples were collected in heparinized tubes via a different cephalic vein predose and 5, 10, 20, 30, 45, 60, 90, 120, 180, 240, and 300 min postdose. Then, the dogs were subsequently used for pharmacokinetic analysis following multiple intravenous doses (base, 0.3 mg/kg, once a day for 7 days) of vonoprazan acetate.

All blood samples were centrifuged for 5 min at $8000 \times g$ to obtain plasma. The plasma samples and homogenates were stored at −80 ℃ until analysis. The concentrations of vonoprazan in the plasma and tissue homogenate were measured using liquid chromatography mass spectrometry (LC–MS)/MS (Supplementary Information).

Kinetics of M-I formation in rat, dog, and human hepatic microsomes
Several studies have demonstrated that the primary metabolite of vonoprazan is mainly M-I and that M-I is further metabolized into M-II. M-I and M-II conjugate with glucuronic acid to form M-I-G and M-II-G [1, 9, 11]. Thus, M-I formation was measured to characterize the metabolism of vonoprazan in the hepatic microsomes of rats, dogs, and humans. The hepatic microsomes from six male Sprague Dawley rats were prepared according to previously described methods [16]. The hepatic microsome incubation system (final volume, 200 μL) consisted of a NADPH-generating system (0.5 mM β-$NADP^+$, 10 mM D-glucose-6-phosphate, 1 U/mL glucose-6-phosphate dehydrogenase and 5 mM $MgCl_2$) and hepatic microsome protein (0.2 mg/mL). The final concentrations of vonoprazan were set to 2.5, 5, 10, 20, and 40 μM for the rat microsomes, 10, 20, 40, 80, and 160 μM for the beagle microsomes and 5, 10, 20, 40, and 80 μM for the human microsomes. The reaction was started by adding the NADPH-generating system after preincubation at 37 ℃ for 5 min. The reaction was stopped by adding 1 mL ice-cold ethyl acetate at the designed time (10 min for rat, 15 min for dog, 15 min for human). The formation of M-I was measured using LC–MS/MS (Supplementary Information).

Transport of vonoprazan across Caco-2 monolayer
Caco-2 cells from Shanghai Cell Bank of the Chinese Academy of Science (Shanghai, China) were seeded at a density of 1.2×10^5 cm^{-2} on a 12-well Millicell hanging insert and left to grow for 21 days to reach confluence. The culture medium was replaced every other day. The integrity of the Caco-2 cell monolayers was
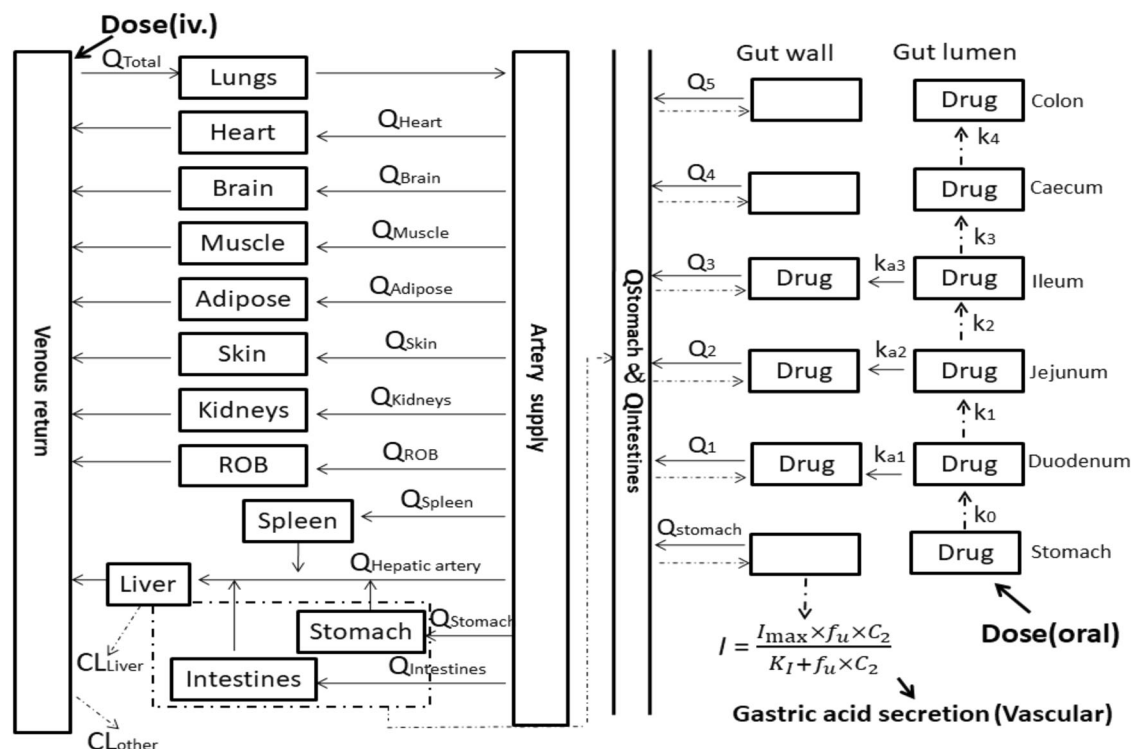
Prediction of vonoprazan PK and PD using PBPK-PD model
WM Kong et al.

854

Fig. 1 Schematic structure of the whole-body PBPK-PD for predicting the pharmacokinetic behaviors of vonoprazan and its inhibition of gastric acid secretion following intravenous or oral administration to rats, dogs, and humans. The antisecretory effect of vonoprazan on gastric acid is linked to the stomach. ROB and Q represent the rest of the body and the blood flow rate, respectively

examined by measuring the trans-epithelial electrical resistance with a Millicell voltammeter (Millicell ERS-2, Merck Millipore, Billerica, MA, USA). On day 21 following culture, the Caco-2 cell monolayers were washed with Hank's balanced salt solution (HBSS, pH 7.4). Then, 50 μM vonoprazan was administered to the apical side (AP, 0.4 mL). The basolateral (BL, 0.60 mL) side served as the receiving chamber and was filled with blank HBSS at 37 °C. One hundred microliters of solution was taken from the BL side at 15, 30, 60, 90, and 120 min and supplemented with 100 μL of blank HBSS. The transported amount of vonoprazan was measured by LC–MS/MS. The permeability coefficient ($P_{app, caco-2}$) in the Caco-2 cells was estimated according to the following equation:

$$P_{app,caco-2} = \frac{\Delta Q}{\Delta t \times A \times C_0},$$ (1)

where ΔQ and Δt represent the amount of vonoprazan that passes through a single cell layer and the time required to do so, respectively. A represents the area of the Transwell chambers. C_0 represents the initial concentration of the drug in the donor pool.

PBPK model development
A PBPK-PD model (Fig. 1) was developed to simulate the pharmacokinetic behavior and efficacy of vonoprazan. The PBPK model consists of the lungs, heart, brain, muscle, adipose, skin, kidneys, arterial blood, venous blood, liver, stomach, intestines, and the rest of the body. Vonoprazan efficacy is directly linked to the stomach. All tissues except for the stomach are represented by a perfusion-rate limited model.

The disposition of vonoprazan in the general tissue compartment is described as follows:

$$V_t \frac{dC_t}{dt} = Q_t \times \left(C_{artery} - \frac{C_t}{K_{t:p}/R_b} \right),$$ (2)

where V_t, C_t, Q_t, and $K_{t:p}$ represent the volume, vonoprazan concentration, blood flow rate, and the tissue-to-plasma vonoprazan concentration ratio in the ith tissue, respectively. R_b represents the blood-to-plasma vonoprazan concentration ratio. Here, R_b was assumed to be 0.91, which was derived from previous report [1].

Pre-experimental results showed that a two compartment model was better fitted to plasma concentration–time data following intravenous dose administration to rats. The estimated $t_{1/2\alpha}$ and $t_{1/2\beta}$ (calculated with the compartment model) of vonoprazan in the rats were 1.53 and 49.85 min, respectively, indicating that drug equilibrium between tissue and plasma occurred at 180 min following intravenous dose administration. The $K_{t:p}$ of vonoprazan in the rats was estimated using the ratio of the vonoprazan concentration at the tissue-to-plasma drug equilibrium between the tissue and the plasma following intravenous dose administration [17]. Due to large species differences in f_u, it was assumed that the ratios of tissue-to-plasma free concentration were identical across species [18]. The $K_{t:p}$ values in other species were estimated by the equation $K_{t:p} = f_u \times K_{t:p,rat}/f_{u,rat}$ [19], where f_u and $f_{u,rat}$ represent the free fraction of vonoprazan in the plasma of the indicated species and in rats, respectively. The values of f_u were 0.32 (rat), 0.17 (dog), and 0.15 (human), respectively [1].

The disposition of vonoprazan in the venous blood compartment is described as follows:

$$V_{vein} \frac{dC_{vein}}{dt} = \sum_t \left(Q_t \times \frac{C_t}{K_{t:p}/R_b} \right) - Q_{total} \times C_{vein} - CL_{other} \times C_{vein},$$ (3)

where Q_{total} and V_{vein} represent the cardiac output and volume of venous blood. Several studies have demonstrated that vonoprazan is eliminated mainly via a metabolism mechanism [1, 9]. Our

Prediction of vonoprazan PK and PD using PBPK-PD model
WM Kong et al.

855

pre-experimental results showed that the CL values of vonoprazan in rats were higher than the hepatic blood flow rates, indicating that vonoprazan metabolism was performed in other tissues, whose clearances were defined as other clearances (CL_{other}). The CL_{other} in rats and dogs were calculated as follows [20, 21]:

$$CL_{other} = CL_{vivo} - \frac{Q_{liver} \times PBSF \times f_u \times V_{max,M-I}/K_{m,M-I}}{Q_{liver} + PBSF \times f_u \times V_{max,M-I}/K_{m,M-I}}, \qquad (4)$$

where the in vivo clearances (CL_{vivo}) in rats and dogs were estimated following intravenous vonoprazan administration to rats (0.5 mg/kg) and dogs (0.3 mg/kg). $V_{max,M-I}$ and $K_{m,M-I}$ represent the maximum rate of M-I formation and the vonoprazan concentration at half the maximum rate of M-I formation, respectively. Moreover, CL_{liver} was estimated using M-I formation, and other vonoprazan metabolism routes also contributed to CL_{other}. Theoretically, CL_{other} is attributed both to the other metabolism routes and to extrahepatic metabolism. PBSF (physiologically based scaling factor) represents the amount of hepatic microsomal protein, which is equal to the amount of microsomal protein times the weight of the liver. The PBSF values were 409.92 (rat), 16592.7 (dog), and 82,472 (human) mg protein/body [19].

Both rat and dog data were used to attempt to scale-up CL_{other} for human; although the estimation failed with the rat data, good predictions were obtained with the dog data. Therefore, dog data were used to scale-up the human CL_{other} via an allometric equation [19], i.e., the values were estimated at 25, 150, and 616 mL/min in rats, dogs and humans, respectively, using the following equation:

$$CL_{other,human} = CL_{other,dog} \times \left(\frac{W_{human}}{W_{dog}}\right)^{0.67}, \qquad (5)$$

where W_{human} and W_{dog} represent the body weight of human and dog, respectively.

The disposition of vonoprazan in the arterial blood compartment and the lung is described by Eqs. (6) and (7), respectively.

$$V_{artery} \frac{dC_{artery}}{dt} = Q_{total} \times \left(\frac{C_{lung}}{K_{lung:p}/R_b} - C_{artery}\right), \qquad (6)$$

$$V_{lung} \frac{dC_{lung}}{dt} = Q_{total} \times \left(C_{vein} - \frac{C_{lung}}{K_{lung:p}/R_b}\right). \qquad (7)$$

The disposition of vonoprazan in the liver is described by Eq. (8).

$$
\begin{aligned}
V_{liver} \frac{dC_{liver}}{dt} = {}& Q_{hepatic} \times C_{artery} + Q_{stomach} \times \frac{C_{stomach}}{K_{stomach:p}/R_b} \\
& + Q_{intestines} \times \frac{C_{intestines}}{K_{intestines:p}/R_b} + Q_{spleen} \times \frac{C_{spleen}}{K_{spleen:p}/R_b} \\
& - Q_{liver} \times \frac{C_{liver}}{K_{liver:p}/R_b} - PBSF \times CL_{liver},
\end{aligned}
\qquad (8)
$$

$$CL_{liver} = CL_{M-I} = \frac{V_{max,M-I} \times f_u \times C_{liver}/K_{liver:p}}{K_{m,M-I} + f_u \times C_{liver}/K_{liver:p}}, \qquad (9)$$

$$E = \frac{f_u \times PBSF \times V_{max,M-I}/K_{m,M-I}}{Q_{liver} + f_u \times PBSF \times V_{max,M-I}/K_{m,M-I}}, \qquad (10)$$

$$K_{liver:p} = \frac{(K_{liver:p})_{obs}}{1 - E}, \qquad (11)$$

where Q_{liver} represents the blood flow rate in the hepatic artery, which equals $Q_{stomach} + Q_{spleen} + Q_{intestines} + Q_{hepatic}$. The $K_{liver:p}$ of vonoprazan in rats was corrected by the liver extraction ratio (E).

The stomach is the target of vonoprazan, several studies have demonstrated that high accumulation of vonoprazan occurs in the stomach [3, 13]. A permeability-limited model was introduced to illustrate the disposition of vonoprazan in the stomach wall

$$V_1 \frac{dC_1}{dt} = Q_{stomach}(C_{artery} - C_1) - PS(C_1 - C_2/K_{stomach:p}), \qquad (12)$$

$$V_2 \frac{dC_2}{dt} = PS(C_1 - C_2/K_{stomach:p}), \qquad (13)$$

where C and V represent the concentration of vonoprazan and the compartment volume, respectively. Subscripts 1 and 2 represent the vascular and extravascular compartments, respectively. We assumed that the ratio of V_1 to V_2 was equal to the ratio of the means of those values from all the tissues [22, 23]. The values of V_1 and V_2 were estimated by the ratio in rat (V_1, 0.2 mL; V_2, 0.9 mL), dog (V_1, 4.6 mL; V_2, 19.4 mL) and human (V_1, 25.6 mL; V_2, 134.4 mL), respectively. PS is the permeability-surface product, which was estimated by fitting this value to the stomach concentration data in rat. The specific reasons for this are described in reference [19]. The values of PS in other species were estimated by Eq. (14).

$$PS_i = PS_{rat} \times \left(\frac{W_i}{W_{rat}}\right)^{0.67}, \qquad (14)$$

where W_i was the weight of the indicated species.

For oral administration, intestinal absorption and intestinal transit processes are introduced into the PBPK model.

It is generally accepted that drug absorption and metabolism in the stomach tract were negligible due to low blood flow, short residence time and the small absorption area. Moreover, vonoprazan in the stomach is highly ionized (pKa: 9) [1], although its targeted organ is the stomach. The amount (A_0) of vonoprazan remaining in the stomach is governed by the constant (k_0) of the gastric emptying rate, i.e.

$$\frac{dA_0}{dt} = -k_0 \times A_0. \qquad (15)$$

The small intestinal tissues were divided into the duodenum, jejunum, ileum, cecum, and colon. It was assumed that drug absorption only occurred in the duodenum, jejunum and ileum. The amount (A_i) of vonoprazan in the gut lumen is described by Eq. (16).

$$\frac{dA_i}{dt} = k_{i-1} \times A_{i-1} - k_i \times A_i - k_{a,i} \times A_i, \qquad (16)$$

where, $i = 1, 2, 3, 4,$ and 5 represent the duodenum, jejunum, ileum, cecum, and colon, respectively. k_i and $k_{a,i}$ represent the constant of gut transit time and the absorption constant of the vonoprazan absorption rate, respectively. The $k_{a,i}$ value of vonoprazan in the duodenum, jejunum and ileum was estimated using Eq. (17) [24].

$$k_{a,i} = \frac{2 \times P_{eff}}{r_i}. \qquad (17)$$

where P_{eff} and r_i are the effective permeability coefficient and radius of the corresponding intestines, respectively. P_{eff} ($\times 10^{-4}$ cm·s^{-1}) is derived from data ($P_{app,Caco-2} \times 10^{-6}$ cm·s^{-1}) obtained in Caco-2 cells [25].

For human

$$Log P_{eff,man} = 0.4926 \times Log P_{app,caco-2} - 0.1454, \qquad (18)$$

For rat

$$P_{eff,man} = 3.6 \times P_{eff,rat} + 0.03. \qquad (19)$$

For dog, it is assumed that $P_{eff,dog}$ equals $P_{eff,man}$. The values of P_{eff} were 0.002 (rat), 0.008 (dog), and 0.008 (human) cm·min^{-1}.

The amount of vonoprazan in the enterocytes (gw) is described by

$$\frac{dA_{gw,i}}{dt} = K_{a,i} \times A_i + Q_{gw,i} \times C_{artery} - Q_{gw,i} \times \frac{C_{gw,i}}{K_{gw:p}/R_b}, \qquad (20)$$

where $Q_{gw,i}$ represents the blood flow rate in the ith intestine segment.

PD model

The stomach is the target of vonoprazan, whose inhibition (I) of gastric acid secretion is directly related to the free vonoprazan concentration in the stomach, i.e.

$$I = \frac{I_{max} \times f_u \times C_2}{K_I + f_u \times C_2}, \qquad (21)$$

where I_{max} and K_I are the maximal inhibition of gastric acid secretion (indexed as inhibition rate % or increases in pH) and the free vonoprazan concentration at 50% maximal inhibition, respectively. It is assumed that the inhibition of gastric acid secretion by vonoprazan is similar across species. The K_I value was set to 35 nM, derived from rabbit gastric H^+/K^+ ATPase-rich vesicles at pH 6.5 [13].

Vonoprazan has been reported to possess a slow dissociation rate from H^+/K^+ ATPase [4]; thus, the inhibitory effects on gastric acid secretion was rewritten as

$$\frac{dI}{dt} = k \times f_u \times C_2 \times (I_{max} - I) - k_d \times I, \qquad (22)$$

where k_d and k are the rate constants of vonoprazan dissociation from H^+/K^+ ATPase and vonoprazan-H^+/K^+ ATPase binding, respectively. k_d was estimated to be 0.00246 min^{-1} using the half-life (4.7 h) of vonoprazan dissociation from H^+/K^+ ATPase expressed in HEK293 cells [4]. k was calculated to be 0.07028 $min^{-1} \cdot \mu M^{-1}$ using the ratio of k_d to K_I (Supplementary information).

Coding and solving of the PBPK-PD model were conducted on WinNonlin 8.1 (Pharsight, St. Louis, MO, USA) using the parameters listed in Table 1 and corresponding code (human, oral) listed in the Supplementary information. The pharmacokinetic profiles of vonoprazan in the plasma of rats, dogs, and humans in the study were predicted, and its parameters were estimated using noncompartmental analysis. The predictions were compared with observed data. Fold errors were used for assessing successful predictions, defined as the ratio of observed data to predicted data when predicted data < observed data, and the ratio of predicted data to observed data when predicted data > observed data. The predictions were considered acceptable if the fold errors were within 2 [26, 27].

Table 1. Physiological parameters used in the PBPK model

	Rat (0.25 kg)			Dog (8.5 kg)			Human (70 kg)		
	Volume[a] (mL)	Blood flow[b] (mL/min)	$K_{t:p}$	Volume[a] (mL)	Blood flow[b] (mL/min)	$K_{t:p}$	Volume[a] (mL)	Blood flow[b] (mL/min)	$K_{t:p}$
Lungs	1.25	83.9	103.76	85	968.33	55.12	1170	5600	48.64
Heart	0.83	4.07	6.78	43	43.3	3.60	310	240	3.18
Brain	1.43	1.66	0.85	50	145	0.45	1450	700	0.40
Muscle	101.00	23.10	5.58	4250	170	2.97	35000	750	2.62
Adipose	19.00	5.82	0.27	1500	50	0.14	10000	260	0.13
Skin	47.50	4.82	2.28	364	18.33	1.21	7800	300	1.07
Kidneys	1.83	11.71	24.63	97	170	13.09	280	1240	11.55
Spleen	0.50	1.66	22.93	22	13.33	12.18	190	80	10.75
Stomach	1.10	1.13	128.67	24	10	68.36	160	38.33	60.31
Liver	9.15	12.30	12.07	213	323.33	2.89	1690	1518.33	2.89
Vein	13.60	/	/	284	/	/	3470	/	/
Artery	6.80	/	/	141	/	/	1730	/	/
Rest of body	36.03	20.42	0.01	1223	48.33	0.01	5100	592	0.01
Duodenum	0.48	0.36	5.19	18	13.5	2.76	70	118	2.43
Jejunum	5.36	4.03	5.19	120	90	2.76	209	413	2.43
Ileum	0.12	0.09	5.19	6	4	2.76	139	244	2.43
Cecum	1.55	1.16	5.19	13	90.5	2.76	116	44	2.43
Colon	2.5	1.88	5.19	46	57	2.76	1116	281	2.43
r_1 (cm)[c]	0.2			0.5			2.00		
r_2 (cm)[c]	0.2			0.5			1.63		
r_3 (cm)[c]	0.2			0.5			1.45		
k_0 (min^{-1})[d]	0.034			0.067			0.08		
k_1 (min^{-1})[d]	0.48			0.0074			0.07		
k_2 (min^{-1})[d]	0.301			0.0074			0.03		
k_3 (min^{-1})[d]	0.020			0.0074			0.04		
k_4 (min^{-1})[d]	ND			ND			0.003		
k_5 (min^{-1})[d]	ND			ND			0.001		

[a]Most values were from refs. [19, 39]; volumes of stomach and intestines were estimated by ratio of length (rat [40], dog [34, 41], and human [24]). Volume of rest of body equaled to total body volume subtracted by the summed volume of listed organs and value of Kt:p was assumed as 0.01
[b]Most values were from refs. [19, 39]; blood flow of stomach and intestines were estimated by ratio of length (rat [40], dog [19, 42, 43], and human [24])
[c]Data in rat [33], dog [34], and human [35]
[d]Data in rat [36] and human [24, 35]. Values in dog and k_0 in human were calculated by fomula and transit time in [34, 37, 38]. ND meant no detected

Prediction of vonoprazan PK and PD using PBPK-PD model
WM Kong et al.

857

Visual predictive checks of the model in human
Visual predictive checks of the method were used to assess the accuracy of the predicted pharmacokinetic profiles and inhibition effects following oral single-dose or multidose administration of 20 mg vonoprazan to the humans. It was assumed that there was interindividual variability in the pharmacokinetic parameters (such as CL_{liver}, f_u) and the PD parameters (k) using the single dose data. The first order conditional estimation of the Lindstrom–Bates (FOCE L–B) method was used in the simulation. The specific method is described in reference [19]. First, for the pharmacokinetic study, the variances of CL_{liver} and f_u (regarded as random effect parameters) together with the standard deviation of the intraindividual error were estimated using four sets of the observed plasma concentration-time profiles in human [5, 28]. Similarly, for the PD study, the variances of CL_{liver}, f_u and k were also estimated using six sets of PD data in human [5, 14, 29]. Then, simulation and verification of the population model were performed on WinNonlin 8.1 (Pharsight, St. Louis, MO, USA). The visual predictive checks were based on 1000 simulations. The 5th, 50th, and 95th percentiles of the simulations were plotted along with the observed data for visual inspection. Pharmacokinetics [14] and PDs [14, 15, 29] data from multidose vonoprazan administration were acquired from the literature.

Data source for vonoprazan
Most of the vonoprazan pharmacokinetic profiles in rats and dogs were obtained in this study. Some data came from the literature [30, 31]. The inhibitory effects of vonoprazan on gastric acid secretion in rats [12] and dogs [30] were cited from PubMed. The pharmacokinetic data for vonoprazan and its inhibitory effects on gastric acid secretion mainly came from data reported in PubMed following oral single-dose or multidose administration to healthy subjects [5, 14, 15, 28, 29, 32].

RESULTS

Kinetics of M-I formation in hepatic microsomes and transport of vonoprazan across Caco-2 monolayers
The formation kinetics of M-I from vonoprazan in rat, dog, and human hepatic microsomes were investigated (Supplementary Fig. S2). The results showed that the formation of M-I fit to Michaelis–Menten equation. The estimated $V_{max,M-I}$ values in the hepatic microsomes of rats, dogs, and humans were 1.50, 0.16, and 0.24 $nmol \cdot min^{-1} \cdot mg^{-1}$ protein, respectively. The corresponding $K_{m,M-I}$ values were 12.94 (rat), 90.97 (dog), and 13.60 (human) μM. Large species variations in the characteristics of M-I formation were observed. The affinity of vonoprazan in the rat hepatic microsomes was similar to that in humans and higher than that in dogs. Vonoprazan transport across the Caco-2 monolayer was documented (Supplementary Fig. S2). The estimated $P_{app,Caco-2}$ of vonoprazan across the Caco-2 monolayer was $3.46 \times 10^{-6} \pm 1.07 \times 10^{-6}$ $cm \cdot s^{-1}$ ($n = 6$). Thus, the values of P_{eff} of vonoprazan across the intestine of rats, dogs, and humans were estimated to be 0.002, 0.008, and 0.008 cm/min, respectively, using Eqs. (18) and (19).

In rat
The pharmacokinetic profiles of vonoprazan in rats (Fig. 2) were investigated following intravenous single-dose (0.5, 1.0, and 2.0 mg/kg), oral (2.0 mg/kg), and intravenous multidose administration (1.0 $mg \cdot kg^{-1} \cdot d^{-1}$ for 7 days), and the corresponding parameters were estimated (Table 2) using noncompartmental analysis. The results showed that the pharmacokinetics of vonoprazan following intravenous dose administration could be characterized as dose-dependent, with CL values following intravenous doses of 0.5, 1.0, and 2.0 mg/kg estimated to be 128.57 ± 12.24, 138.80 ± 2.75, and 77.23 ± 4.67 $mL \cdot min^{-1} \cdot kg^{-1}$, respectively. Moreover, these CL values were higher than that for hepatic blood flow (49.2 $mL \cdot min^{-1} \cdot kg^{-1}$), indicating the existence of extrahepatic metabolism. The estimated

clearance of the extrahepatic metabolism was 100 $mL \cdot min^{-1} \cdot kg^{-1}$ using data from intravenous dose administration (0.5 mg/kg) and Eq. (4). A high distribution volume (6.32–10.88 L/kg) of vonoprazan was also observed in rats, which exceeded the body volume tenfold, indicating that special tissue distribution occurred. The plasma concentration profiles and pharmacokinetic parameters of vonoprazan following multidose administration were similar to those following single-dose administration, indicating that no accumulation occurred. The compound could be absorbed, but its bioavailability was approximately 9%, which was consistent with a previous report [1].

The plasma pharmacokinetic profiles of vonoprazan following intravenous single or oral dose administration to rats were predicted using the developed PBPK model (Fig. 2a–c). The corresponding pharmacokinetic parameters were compared with the observed data (Table 2). During the predictions, the distribution of vonoprazan in the stomach was depicted using a limited-membrane model. The PS value of vonoprazan in the rat stomach was estimated to be 0.6 mL/min based on the vonoprazan distribution data. The PS values in the stomach of dogs and humans were also calculated to be 6.37 and 26.17 mL/min, respectively, using Eq. (14). The results showed that most (11/13) of the predicted exposure parameters (including AUC_{0-tn} and C_{max}) were between 0.5- and 2.0-times those of the observed data (Table 2) following intravenous and oral dose administration.

The distribution kinetics of vonoprazan in the heart, liver, spleen, lungs, stomach, intestines, brain, kidneys, muscle, skin, and adipose following intravenous dose administration (1 mg/kg) to rats were also predicted and compared with the observations (Fig. 3). The results showed that the predicted data were in good agreement with the observed data except in the skin and spleen. The tissue concentration tended to be underestimated, which might be related to the overestimation of the plasma concentration (Fig. 3l). Remarkably high concentrations of vonoprazan were observed in the above indicated tissues, especially in the stomach, heart, lungs, kidneys, and intestines, which was consistent with the high apparent distribution volume of vonoprazan. Different from other tissues, the vonoprazan concentration–time profile in the stomach did not synchronize with that in the plasma. The concentration of vonoprazan in the stomach exhibited an obvious increase, although plasma concentrations rapidly decreased, with time, which was successfully depicted by a permeability-limited model.

The stomach is the targeted tissue of vonoprazan. The concentrations of vonoprazan (Fig. 2e) in the stomach and its inhibitory effects on gastric acid secretion (Fig. 2f) following single intravenous doses (0.5, 0.7, and 1.0 mg/kg) to rats were simultaneously predicted. The inhibitory effects on gastric acid secretion were indexed as alterations in pH values. The basal pH and I_{max} were set to 2.0 and 4.0, respectively. The predicted pH values following intravenous administration of vonoprazan to rats were compared with data reported previously in anesthetized rats indexed as the pH of gastric perfusate induced by histamine stimulation [12]. The results showed that the predicted increases in pH by vonoprazan administration were consistent with observations following intravenous administration of 0.7 and 1.0 mg/kg vonoprazan (Fig. 2f, g).

The inhibitory effects were sustained for 5 h after intravenous administration. The predicted vonoprazan concentrations in the stomach 5 h following intravenous single-dose administration (0.7 and 1.0 mg/kg) to rats were 1043 and 1490 ng/g, respectively (Fig. 2e), which were more than 4000-fold higher than those in plasma (0.25 and 0.35 ng/mL, respectively), indicating that the long-lasting inhibitory effect of vonoprazan on gastric acid secretion was associated with its high concentration in the stomach instead of that in the plasma. Most of the predicted pH values were within 1.5-fold error compared with the observations (Fig. 2g). However, the increases in pH were overpredicted in the rats treated with the low dose (0.5 mg/kg) of vonoprazan.
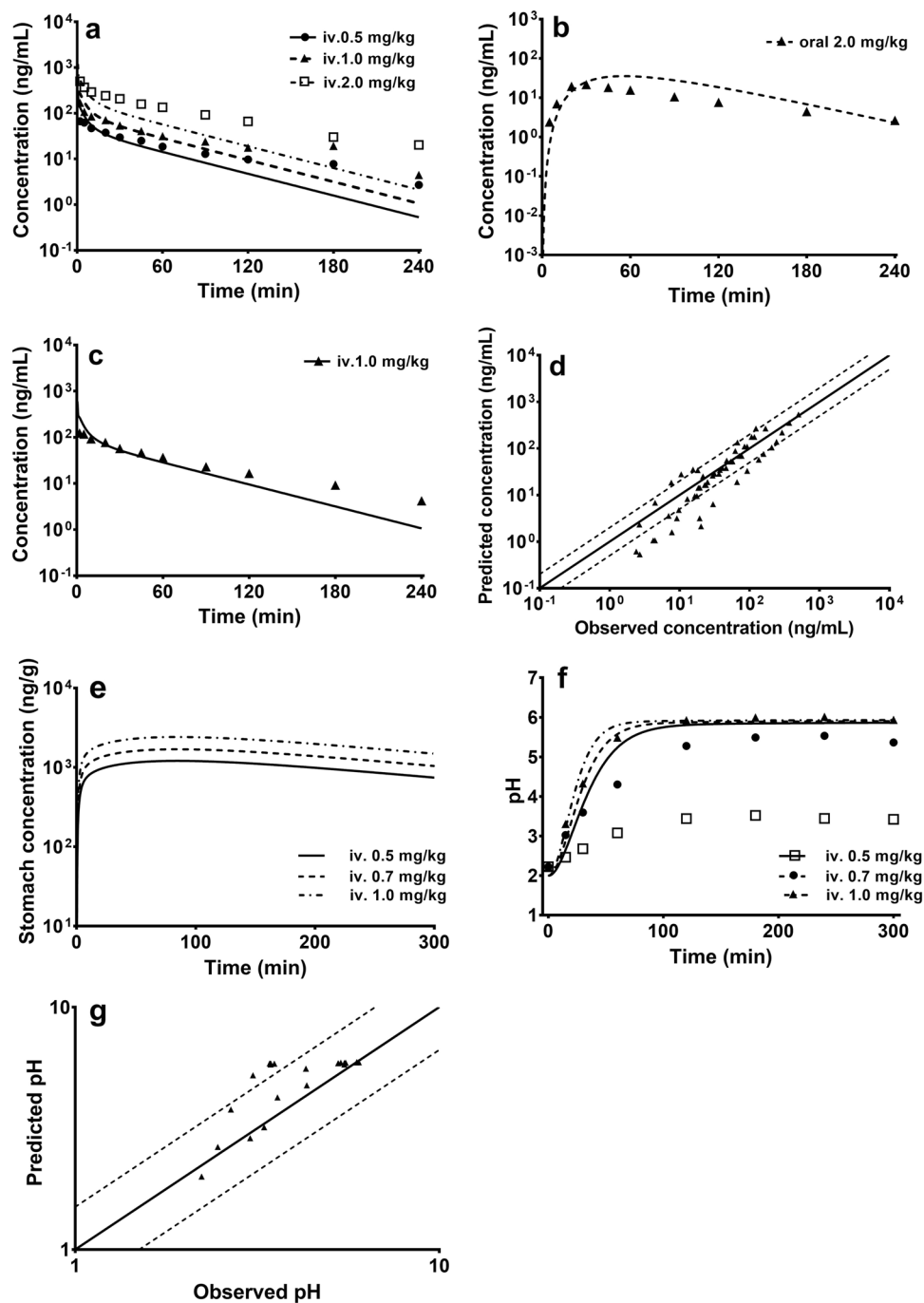
Prediction of vonoprazan PK and PD using PBPK-PD model
WM Kong et al.

858

Fig. 2 The predicted results in rats. The predicted (lines) and observed (points) vonoprazan concentration in the plasma of rats following intravenous dose (**a** 0.5, 1.0, 2.0 mg/kg, $n = 5$), oral dose (**b** 2.0 mg/kg, $n = 5$), and multidose (**c** 1.0 mg/kg for 7 days, $n = 5$) administration. **d** The relationship between the mean observed and predicted concentrations of vonoprazan in the plasma of rats. The solid and dashed lines indicate unity and twofold errors between predicted and observed data, respectively. **e** The simulated concentration of vonoprazan in the stomach of rats following intravenous administration at 0.5, 0.7, and 1.0 mg/kg, respectively. **f** The predicted increases (lines) in gastric pH and the observations (points) following administration of the corresponding doses of vonoprazan. **g** The relationship between the observed and predicted pH levels of the stomach. The solid and dashed lines indicate unity and 1.5-fold errors between predicted and observed data, respectively. The observations were obtained from the literature [12] and were induced by intravenous infusions of histamine

In dog
The pharmacokinetic profiles of vonoprazan in the beagles following intravenous single-dose administration (0.15, 0.3, and 0.6 mg/kg), oral administration (0.6 mg/kg) and intravenous multi-dose administration (0.3 mg·kg⁻¹·d⁻¹ for 7 days) of vonoprazan were documented (Fig. 4a–c and Table 3). Similar to the findings in rats, the pharmacokinetics of vonoprazan in dogs also showed

dose-dependent characteristics. The CL values following intravenous doses of 0.15, 0.30, and 0.60 mg/kg vonoprazan were estimated to be 23.00 ± 2.61, 18.26 ± 3.92, and 12.92 ± 2.95 mL·min⁻¹·kg⁻¹, respectively. The calculated CL_{other} value was 17.65 mL·min⁻¹·kg⁻¹ based on an intravenous dose of 0.30 mg/kg vonoprazan. Different from rats, the distribution volumes of vonoprazan (1.17–1.31 L/kg) in the dogs were similar

Prediction of vonoprazan PK and PD using PBPK-PD model
WM Kong et al.

859

Table 2. Observed and predicted plasma pharmacokinetics parameters in rat following intravenous administration (iv.) and oral administration (oral)

Dose mg/kg	$t_{1/2}$ (min)		AUC_{0-tn} (min*µg/mL)		CL (mL·min^{-1}·kg^{-1})		V_{ss} (L/kg)	
	obs.	pre.	obs.	pre.	obs.	pre.	obs.	pre.
iv. 0.5	66.11 ± 12.52	37.88	3.65 ± 0.33	3.21	128.57 ± 12.24	154.40	10.62 ± 1.28	6.30
iv. 1.0	60.10 ± 9.54	37.88	6.82 ± 0.19	6.42	138.80 ± 2.75	154.38	10.88 ± 1.24	6.30
iv. 2.0	61.64 ± 5.19	37.70	24.16 ± 1.41	12.84	77.23 ± 4.67	154.33	6.32 ± 0.46	6.30
iv. 0.75[b]	72.00 ± 0.00	37.33	5.94 ± 0.24	4.81	NR	154.41	NR	6.30
iv. 1.0 (multidose)	59.20 ± 7.25	37.83	6.70 ± 1.27	6.42	145.58 ± 25.17	154.34	10.57 ± 1.01	6.30
					T_{max} (min)		C_{max} (ng/mL)	
oral. 2.0	70.16 ± 11.62	40.88	2.16 ± 0.49	3.90	26.00 ± 5.50	55.5	21.80 ± 8.23	35.52
oral. 2.0[a]	78 ± 6	40.88	1.62 ± 0.18	3.90	18 ± 0	55.5	17 ± 3	35.52
oral. 1.57[b]	112.2 ± 49.8	43.63	2.60 ± 1.03	3.06	42.6 ± 25.8	55.5	21.19 ± 3.52	27.85
oral. 3.14[b]	118.2 ± 49.2	59.52	9.03 ± 2.76	6.13	49.8 ± 36.6	55.5	73.27 ± 13.35	55.93

NR no reported, *Obs.* observed, *pre.* predicted
Data of [a] and [b] were from [30] and [31], respectively

to the body weight, implying that vonoprazan was mainly distributed in the body fluids, which was consistent with the low free fraction in the plasma. Moreover, good absorption of vonoprazan was found in the dogs, and the estimated bioavailability was 70%, which was near the 52% reported previously [1]. No obvious accumulation occurred following intravenous multidose administration of vonoprazan.

The developed PBPK model for the rats was also extrapolated for the dogs for predicting the pharmacokinetic profiles of vonoprazan (Fig. 4a–d) following intravenous or oral administration. Good predications were also obtained. Among the 24 predications of the pharmacokinetic parameters, 22 (approximately 92%) were within twofold errors of the observations (Table 3). The predicted bioavailability (approximately 56%) was also close to that of the observations (approximately 70%).

The vonoprazan concentration (Fig. 4e) in the stomach and its inhibition of gastric acid secretion (Fig. 4f) following oral administration of 0.1, 0.3, and 1.0 mg/kg vonoprazan to the Heidenhain pouch in dogs were also predicted (Table 3). Inhibition of acid output (% of predose levels) was indexed as the PDs, and I_{max} was set to 100%. The results showed that the predicted inhibition (Fig. 4f, g) of gastric acid secretion following oral administration of 0.3 and 1.0 mg/kg vonoprazan were comparable to the observed results induced by a subcutaneous injection of histamine (30 µg/kg) [30]. The inhibition effects lasted for 24 h after the dose administration. The predicted gastric acid secretions 24 h following administration of the above two doses were 48% and 26% of the predose levels, while the concentrations of vonoprazan in the stomach were predicted to be 52.31 and 174.39 ng/g, respectively, more than 30,000-fold higher than those in the plasma (0.0016 and 0.0055 ng/mL). Most of the predicted acid output (% of predose levels) were within twofold error, except for the low dose (0.1 mg/kg), compared with the observations (Fig. 4g). These results further demonstrated that the inhibitory effects of vonoprazan on gastric acid secretion were linked to the concentration of vonoprazan in the stomach. However, overpredicted inhibition was found in the dogs treated with 0.1 mg/kg vonoprazan, especially at the first phase.

Prediction of vonoprazan pharmacokinetics and its efficacy using PBPK-PD model in humans
After developing and validating the PBPK-PD model in the rats and dogs, the PBPK-PD model was further extrapolated to predict the pharmacokinetic profiles and efficacies of vonoprazan following oral single-dose and multidose administration of

vonoprazan to 70-kg humans (Fig. 5a–c). CL$_{other}$, was estimated to be 616 mL/min according to interspecies allometric scaling from the value in dogs. The predicted CL and V_{ss} of vonoprazan in the humans were 874 mL/min and 228 L, respectively. The predicted pharmacokinetic profiles and pharmacokinetics of vonoprazan following oral single-dose or multidose administration (10, 20, 30, and 40 mg vonoprazan) were compared with those of previous reports [5, 14, 28, 32] (Table 4). The results showed that except for $t_{1/2}$, most of the predicted concentrations and pharmacokinetic parameters were consistent with the observations, whose fold errors were less than 2. The estimated bioavailability was 36%, which was less than that in dogs. The plasma concentration profiles and pharmacokinetic parameters for the single doses were similar to those for the multidose administration, indicating no drug accumulation.

The concentrations of vonoprazan (Fig. 5d) in the stomach and its inhibition (Fig. 5e) of gastric acid secretion following oral single-dose or multidose administration of 10, 20, 30, and 40 mg/kg vonoprazan to the humans were simultaneously predicted and compared with the observed data. It was assumed that the intragastric pH was 7.0 when gastric acid secretion was completely inhibited. The basal pH (predose) was assumed to be 2.0 [14]; thus, I_{max} was set to 5.0. The results showed that the predicted increases in pH values were in line with the observed data following single-dose or multidose administration of 20, 30, and 40 mg vonoprazan. The acid inhibition effect of vonoprazan persisted for 24 h. In the first 4 h following multidose administration, the predicted increases in the pH values were higher than those following single-dose administration at each corresponding time point, which was in line with the observed data. The predicted concentrations of vonoprazan in the stomach were greater than 1000-times higher than those in the plasma 24 h after oral administration of vonoprazan. Moreover, accumulation of vonoprazan occurred in the stomach following multidose administration, although this was not observed in the plasma. Overpredictions of pH levels were observed in subjects treated with 10 mg vonoprazan, especially during the night-time period, from 12 to 20 h following dose administration.

Visual predictive checks of the model in humans
Visual predictive checks of the model for the pharmacokinetic profiles of vonoprazan and its antisecretory effects on gastric acid following single and multidose administration of vonoprazan (20 mg) to humans were documented (Fig. 5g, h). The observed data came from different clinical reports. The results showed
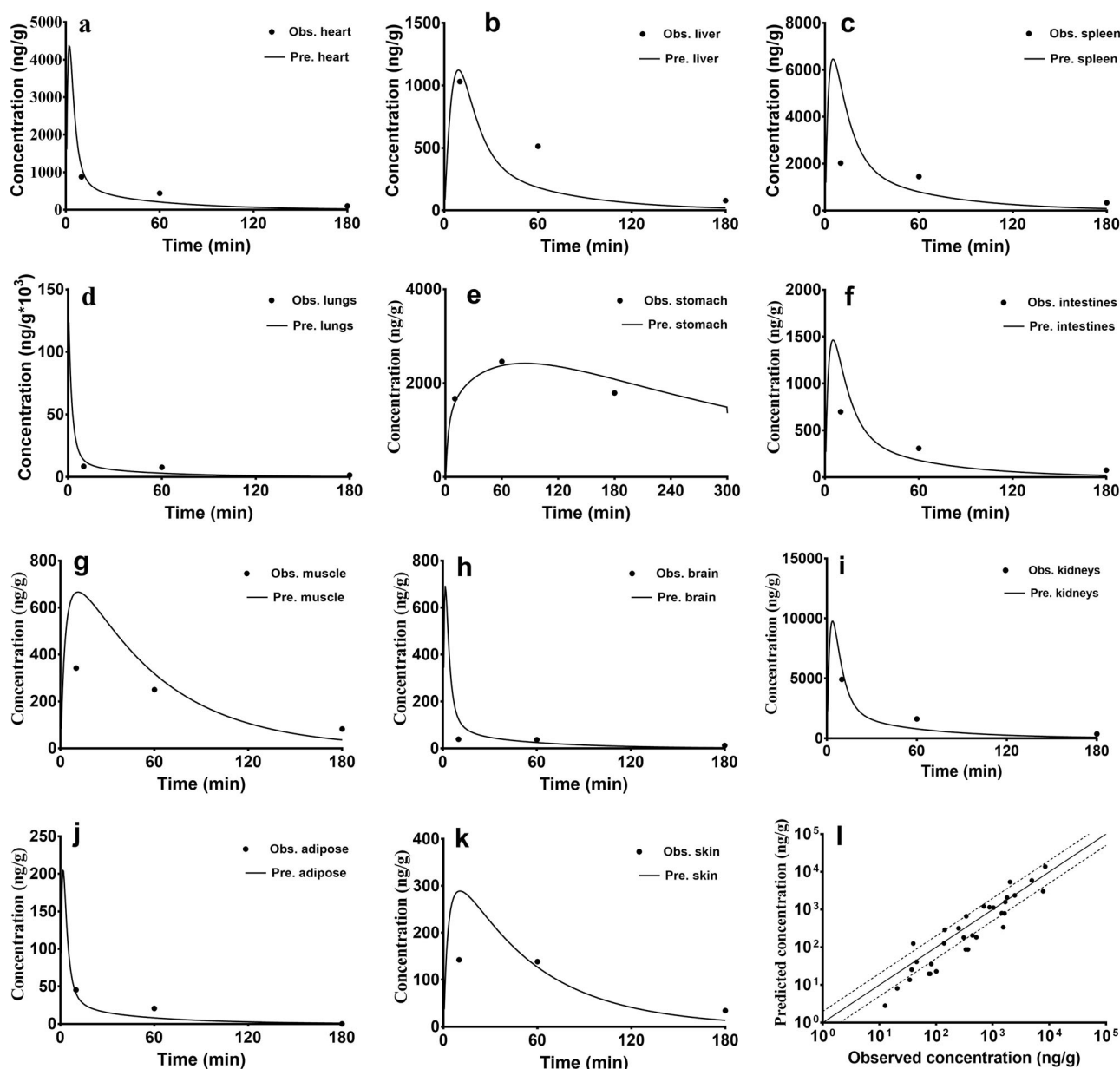
Prediction of vonoprazan PK and PD using PBPK-PD model
WM Kong et al.

860

Fig. 3 The results of tissue distribution in rats. The predicted (lines) and observed (points) vonoprazan concentrations in the heart (**a**), liver (**b**), spleen (**c**), lungs (**d**), stomach (**e**), intestines (**f**), muscle (**g**), brain (**h**), kidneys (**i**), adipose (**j**), and skin (**k**) of rats following intravenous administration of 1 mg/kg vonoprazan ($n = 5$). **l** The relationship between the mean observed and predicted concentrations of vonoprazan in the tissues. The solid and dashed lines indicate unity and twofold errors between predicted and observed data, respectively

that most of the observed data were located between the 5th and 95th percentiles of the simulations, while the median of the observed data approached the 50th percentile of the simulations. These results demonstrated that the deviation between the observed data and the predicted profiles was reasonable, indicating that good predictions of vonoprazan pharmacokinetics and its efficacy in humans were achieved by the developed PBPK-PD model.

DISCUSSION
Vonoprazan possesses a long-lasting inhibitory effect on acid-related disorders. The inhibitory effect on gastric acid secretion seems to be linked to its concentration in the stomach rather than in plasma. The main contribution of the present study was to develop a PBPK-PD model of the stomach to simultaneously predict the

pharmacokinetic behaviors of vonoprazan and its inhibitory effects on gastric acid secretion based on in vitro PD and pharmacokinetic parameters. The developed model was further verified by the observed data from rats, dogs and humans, indicating the potential application of the developed PBPK-PD model.

First, the pharmacokinetic behaviors of vonoprazan in rats and dogs following intravenous or oral administration were predicted using the developed PBPK models based on in vitro pharmacokinetic parameters. In vitro metabolism and transport parameters were obtained from M-I metabolism in hepatic microsomes and transport across Caco-2 monolayers, respectively. Tissue-to-plasma ratios were measured in the rats. The tissue distribution in rats demonstrated that the stomach showed a high distribution of vonoprazan. Moreover, the vonoprazan concentration in the stomach did not synchronize with that in the plasma. The concentration of vonoprazan in the stomach exhibited an obvious
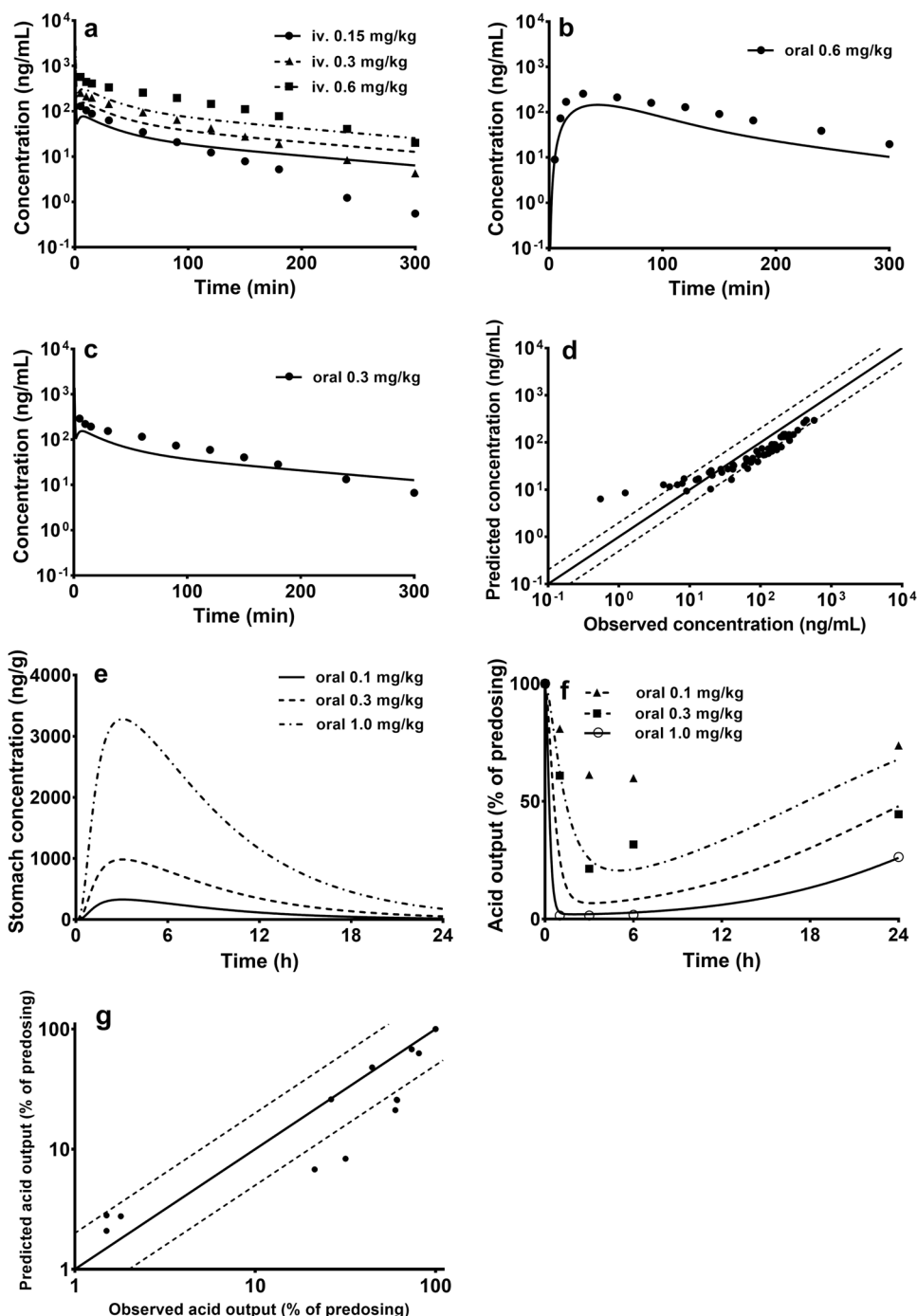
Prediction of vonoprazan PK and PD using PBPK-PD model
WM Kong et al.

861

Fig. 4 The predicted results in dogs. The predicted (lines) and observed (points) vonoprazan concentration in the plasma of dogs following intravenous single-dose administration (**a** 0.15, 0.3, 0.6 mg/kg, $n = 8$), oral administration (**b** 0.6 mg/kg, $n = 8$), and multidose administration (**c** 0.3 mg/kg for 7 days, $n = 8$). **d** The relationship between the mean observed and predicted vonoprazan concentrations in the plasma of dogs. The solid and dashed lines indicate unity and twofold errors between predicted and observed data, respectively. **e** The predicted vonoprazan concentration in the stomach of dogs following oral administration of 0.1, 0.3, and 1.0 mg/kg vonoprazan. **f** The predicted (lines) and observed (points) output of gastric acid (% of predose levels) following oral administration of vonoprazan to dogs. **g** The relationship between the observed and predicted outputs of gastric acid (% of predose levels) in the stomach. The solid and dashed lines indicate unity and twofold errors between predicted and observed data, respectively. The observations of gastric acid output were cited from the literature [30] in the Heidenhain pouches of dogs induced by subcutaneous infusions of histamine

increase, although plasma concentrations decreased, with time. A permeability-limited model was used to illustrate the disposition of vonoprazan in the stomach. It was also found that system clearances of vonoprazan in the rats were higher than the hepatic blood flow, demonstrating the existence of extrahepatic metabolism, which was also introduced into the developed PBPK model.

The results showed that most of the predicted pharmacokinetic profiles and the pharmacokinetic parameters following intravenous or oral administration to the rats and dogs were consistent with the observed data, whose errors were within twofold. In vivo data from the dogs and rats demonstrated dose-dependent pharmacokinetics, which was inconsistent with the predictions. In

Prediction of vonoprazan PK and PD using PBPK-PD model
WM Kong et al.

862

Table 3. The observed and predicted plasma pharmacokinetics parameters in dog following intravenous administration (iv.) and oral administration (oral)

Dose (mg/kg)	$t_{1/2}$ (min)		AUC_{0-tn} (min*µg/mL)		CL (mL·min^{-1}·kg^{-1})		V_{ss} (L/kg)	
	obs.	pre.	obs.	pre.	obs.	pred.	obs.	pre.
iv. 0.15	45.33 ± 8.70	109.36	6.39 ± 0.74	7.31	23.00 ± 2.61	18.04	1.26 ± 0.25	2.18
iv. 0.3	52.18 ± 11.14	109.36	16.66 ± 3.20	14.62	18.26 ± 3.92	18.04	1.31 ± 0.40	2.18
iv. 0.6	61.84 ± 16.53	109.36	46.53 ± 10.07	29.24	12.92 ± 2.95	18.04	1.17 ± 0.29	2.18
iv. 0.1[a]	72 ± 6	109.43	2.64 ± 0.12	4.87	NR	18.04	NR	2.18
iv. 0.3 (multidose)	57.15 ± 7.70	109.38	19.89 ± 7.06	14.63	16.07 ± 4.80	18.03	1.23 ± 0.31	2.18
					T_{max} (min)		C_{max} (ng/mL)	
oral 0.6	65.78 ± 17.31	65.71	31.68 ± 8.15	16.26	31.90 ± 12.50	43.00	266.26 ± 60.85	145.73
oral 0.3[a]	66 ± 6	65.77	4.08 ± 0.96	8.13	NR	43.00	NR	72.86

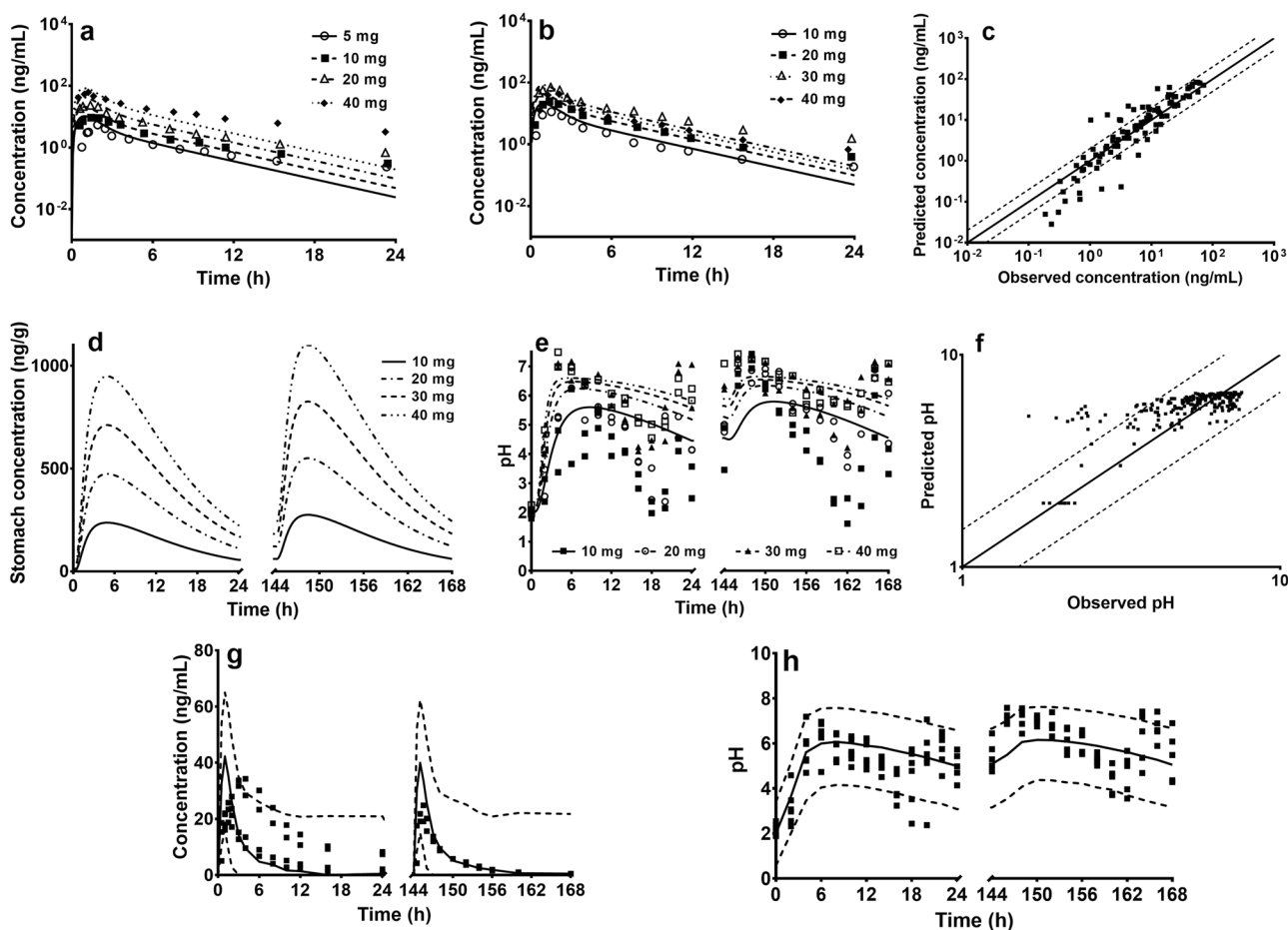[a]The observed values were detected in [30]

Fig. 5 The predicted results in humans. The predicted (lines) and observed (points) vonoprazan concentrations in the plasma of humans following oral single-dose (**a** 5, 10, 20, and 40 mg) and multidose administration (**b** 10, 20, 30, and 40 mg for 7 days). The observed data were cited in the literature [5, 14] in Japanese. **c** The relationship between the mean observed and predicted plasma concentrations of vonoprazan in humans. The solid and dashed lines indicate unity and twofold errors between predicted and observed data, respectively. **d** The predicted vonoprazan concentrations in the stomach of humans following oral single-dose and multidose administration of 10, 20, 30, and 40 mg vonoprazan. **e** The predicted (lines) and observed (points) pH values following oral single-dose or multidose administration of 10, 20, 30, and 40 mg vonoprazan to humans. The observations were cited from literature [14] from Japan and the UK. **f** The relationship between the observed and predicted alterations in pH in the stomach of humans. The solid and dashed lines indicate unity and 1.5-fold errors between predicted and observed data, respectively. **g** Visual predictive checks of the predicted concentrations of vonoprazan following oral single-dose or multidose administration of 20 mg vonoprazan to humans. The observed data were cited from the literature [5, 14, 28]. **h** Visual predictive checks of the predicted alterations in gastric pH following oral single-dose or multidose administration of 20 mg vonoprazan to humans. Solid lines represent the 50th percentiles. Dashed lines represent the 5th and 95th percentiles of the simulated populations. Points represent observed data cited from the literature [5, 14, 15, 29]

Prediction of vonoprazan PK and PD using PBPK-PD model
WM Kong et al.

863

Table 4. The observed and predicted plasma pharmacokinetics parameters in human following oral administration (oral)

	Dose (mg/kg)	$t_{1/2}$ (min)		AUC$_{0-tn}$ (min*μg/mL)		T_{max} (min)		C_{max} (ng/mL)	
		obs.	pre.	obs.	pre.	obs.	pre.	obs.	pre.
Single dose	oral 10 mg[a]	486 ± 90	191.15	3.2 ± 1.3	4.01	90 (45–182)	55	7.9 ± 3.9	20.79
	oral 15 mg[a]	438 ± 66	191.15	6.3 ± 1.4	6.02	90 (90–120)	55	14.0 ± 4.0	31.19
	oral 20 mg[a]	468 ± 66	191.22	8.3 ± 2.4	8.02	90 (60–180)	55	20.0 ± 6.4	41.59
	oral 30 mg[a]	486 ± 60	191.15	15.0 ± 5.7	12.04	90 (60–90)	55	38.6 ± 13.2	62.40
	oral 40 mg[a]	504 ± 54	189.31	25.0 ± 9.5	16.05	105 (45–180)	55	51.8 ± 17.0	83.22
	oral 5 mg[b]	456 ± 66	191.15	1.71 ± 0.56	2.01	90 (60–180)	55	4.2 ± 1.4	10.40
	oral 10 mg[b]	414 ± 60	191.15	3.40 ± 0.50	4.01	105 (60–120)	55	9.7 ± 2.1	20.79
	oral 20 mg[b]	414 ± 48	191.22	8.93 ± 2.11	8.02	90 (45–120)	55	25.0 ± 5.6	41.59
	oral 40 mg[b]	426 ± 30	189.31	26.00 ± 7.55	16.05	90 (60–180)	55	71.9 ± 23.3	83.22
	oral 20 mg[c]	486 ± 82	191.22	17.49 ± 5.61	8.02	240 (90–360)	55	37.53 ± 12.78	41.59
	oral 20 mg[c]	416 ± 41	191.22	15.16 ± 5.10	8.02	180 (60–360)	55	37.99 ± 17.47	41.59
	oral 40 mg[d]	432 ± 64	189.31	22.92 ± 6.12	16.05	120 (30–243)	55	49.5 ± 16.7	83.22
	oral 10 mg[e]	450 ± 78	191.15	4.88 ± 1.88	4.01	90 (45–180)	55	10.9 ± 5.7	20.79
	oral 20 mg[e]	414 ± 96	191.22	10.63 ± 5.77	8.02	90 (45–120)	55	26.2 ± 14.8	41.59
	oral 30 mg[e]	366 ± 24	191.15	15.33 ± 3.19	12.04	90 (45–240)	55	37.2 ± 11.9	62.40
	oral 40 mg[e]	378 ± 36	189.31	25.25 ± 6.45	16.05	90 (45–121)	55	58.5 ± 10.9	83.22
	oral 10 mg[f]	420 ± 114	191.15	3.70 ± 0.81	4.01	90 (45–180)	55	10.1 ± 2.0	20.79
	oral 20 mg[f]	348 ± 60	191.22	7.30 ± 1.97	8.02	90 (90–180)	55	19.5 ± 6.1	41.59
	oral 30 mg[f]	342 ± 42	191.15	13.88 ± 4.36	12.04	90 (60–180)	55	38.8 ± 16.7	62.40
	oral 40 mg[f]	402 ± 108	189.31	23.50 ± 10.57	16.05	90 (45–120)	55	62.0 ± 24.9	83.22
Multidose	oral 10 mg[e]	528 ± 180	180.22	6.3 ± 2.5	4.02	90 (60–120)	55	12.2 ± 4.0	20.83
	oral 20 mg[e]	516 ± 114	180.22	11.7 ± 4.0	8.04	66 (45–120)	55	26.2 ± 10.7	41.67
	oral 30 mg[e]	528 ± 72	180.22	20.3 ± 5.0	12.06	90 (66–240)	55	41.6 ± 11.0	62.52
	oral 40 mg[e]	492 ± 48	180.22	29.3 ± 7.9	16.09	90 (45–240)	55	59.9 ± 15.4	83.38
	oral 10 mg[f]	420 ± 96	180.22	4.77 ± 0.97	4.02	90 (45–180)	55	12.0 ± 1.8	20.83
	oral 20 mg[f]	366 ± 72	180.22	9.10 ± 2.42	8.04	90 (45–180)	55	23.3 ± 6.6	41.67
	oral 30 mg[f]	348 ± 36	180.22	17.47 ± 6.07	12.06	90 (60–120)	55	48.6 ± 17.4	62.52
	oral 40 mg[f]	366 ± 66	180.22	21.51 ± 9.10	16.09	90 (45–180)	55	75.2 ± 25.3	83.38

[a] and [b] came from ref. [5], and volunteers came from UK and Japan, respectively. [c] and [d] were reported in refs. [28] and [32], respectively. [e] and [f] came from ref. [14], and volunteers came from UK and Japan, respectively

vitro metabolic data were derived from M-I formation in hepatic microsomes. The existence of a high amount of extraphepatic metabolism and the contribution of other metabolic routes to the value of CL$_{other}$ may have led to the observed discrepancies between the observations and predictions, which requires further investigation.

The stomach is the target tissue of vonoprazan. Moreover, concentration–time profiles in the stomach did not synchronize with those in the plasma, indicating that the concentration profiles in the stomach are more obviously linked to drug efficacy than those in the plasma. The disposition of vonoprazan in the stomach was also predicted using the developed PBPK model. It was assumed that the inhibitory effects on gastric acid secretion (PD) were linked to the free concentration of vonoprazan in the stomach; therefore, the PBPK-PD model was further introduced to describe the PDs of vonoprazan in both rats and dogs. Vonoprazan shows antisecretory effects on gastric acid via inhibition of H$^+$/K$^+$ ATPase activity. Moreover, vonoprazan is characterized as having a slow dissociation rate from the H$^+$/K$^+$ ATPase-complex. The inhibitory effects of vonoprazan on gastric acid secretion are assumed to be similar across species, and in vivo PD parameters were considered the same as the in vitro parameters [4, 13]. These characteristics of vonoprazan were considered in the PBPK-PD model. Consistent with our

expectations, good predictions were obtained with high and medium doses of vonoprazan (0.7 and 1.0 mg/kg for rats; 0.3 and 1.0 mg/kg for dogs), indicating that it was possible to predict its in vivo inhibitory effects on gastric acid secretion from in vitro PD parameters using the developed PBPK-PD models. However, the reasons for the poor prediction for the low doses of vonoprazan (0.5 mg/kg for rats and 0.1 mg/kg for dogs) were not clear. We also noted that overprediction of gastric acid output following low dose (0.1 mg/kg) administration was associated with overpredicted plasma concentrations of vonoprazan. Moreover, the gastric acid output came from the Heidenhain pouches of the dogs, and the K_I value came from rabbit gastric H$^+$/K$^+$ ATPase-rich vesicles. All of these factors may have led to the overprediction of gastric acid output in the dogs, which requires further investigation.

The PBPK-PD model, following verification in rats and dogs, was further applied to simultaneously predict the pharmacokinetic profiles of vonoprazan and its efficacy in humans. Consistent with our expectations, the pharmacokinetic behaviors of vonoprazan in humans following oral single-dose or multidose administration (10, 20, 30, and 40 mg) were successfully predicted with the exception of $t_{1/2}$; furthermore, most of the predicted concentrations of vonoprazan in the plasma and its pharmacokinetic parameters were within twofold errors. The alterations in

Prediction of vonoprazan PK and PD using PBPK-PD model
WM Kong et al.

864

intragastric pH following single-dose or multidose oral administration were also simulated using the developed PBPK-PD model based on in vitro PD parameters [4, 13]. The results showed that the predicted increases in intragastric pH were in line with the observed data following a single dose or multidose of 20, 30, and 40 mg vonoprazan. Visual predictive checks of the model further demonstrated successful predictions of vonoprazan pharmacokinetics and its efficacy in humans by the PBPK-PD model. The acid suppressant effect of vonoprazan persisted for 24 h. Compared with the single dose, the increases in the pH values prior to administration of the multidose and in the first 4 h afterwards were higher than at the corresponding time points following the single dose. Simulations demonstrated that the concentration of vonoprazan in the stomach at 24 h following oral administration of vonoprazan were 1000-times higher than those in the plasma, and an accumulation of vonoprazan occurred in the stomach following multidose administration, resulting in 24-h suppression of gastric acid secretion in subjects following single-dose administration or sustained suppression of gastric acid secretion throughout each 24-h dosing interval during multidose administration. Moreover, the slow dissociation rate of vonoprazan [4] from the H^+/K^+ ATPase complex also partly explained its long-lasting antisecretory effect. It was also found that the predicted alterations in pH in the subjects were higher than those in the observed data following 10 mg vonoprazan administration, especially during the night-time period, which may be due to nocturnal acid breakthrough. Fortunately, the results of the visual predictive checks of the model in the humans showed that the measured values were basically within the range of predicted values. Furthermore, we hypothesized that the biological rhythm of gastric acid secretion and species variation in the PD parameters of vonoprazan might have led to poor predications, which needs further investigation.

In summary, a PBPK-PD model of the stomach was successfully developed to simultaneously predict the pharmacokinetics and inhibitory effects of vonoprazan on gastric acid secretion following oral or intravenous administration to rats, dogs and humans using in vitro pharmacokinetic and PD parameters. The PBPK-PD model developed for the animals was further extrapolated to make predictions for humans. The predicated plasma concentration of vonoprazan and its anti-gastric acid secretion effects following single-dose and multidose administration of vonoprazan to humans were comparable to the clinical observations, further verifying the clinical application of the developed PBPK-PD model. These findings may highlight the 24-h suppression of gastric acid secretion in subjects following single-dose administration or the sustained suppression of gastric acid secretion throughout each 24-h dosing interval during multidose administration of vonoprazan. In this model, the pharmacokinetic data for intravenous injection and oral administration were predicted, and the efficacy of vonoprazan was predicted from the predicted concentration in the target tissues. In the development of new drugs, when the mechanism is unknown, this PBPK-PD model could be provided for reference.

AUTHOR CONTRIBUTIONS
WMK, BBS, LL, and XDL designed the experiments, analyzed the data, and wrote the paper; WMK, BBS, ZJW, XKZ, KJZ, YC, JXZ, LZ, and PHL conducted the experiments; WMK, BBS, XDL, and LL performed the data analysis; PL, RJX, and LL reviewed the paper.

REFERENCES
1. Kogame A, Takeuchi T, Nonaka M, Yamasaki H, Kawaguchi N, Bernards A, et al. Disposition and metabolism of TAK-438 (vonoprazan fumarate), a novel potassium-competitive acid blocker, in rats and dogs. Xenobiotica. 2017;47:255–66.
2. Echizen H. The first-in-class potassium-competitive acid blocker, vonoprazan fumarate: pharmacokinetic and pharmacodynamic considerations. Clin Pharmacokinet. 2016;55:409–18.
3. Otake K, Sakurai Y, Nishida H, Fukui H, Tagawa Y, Yamasaki H, et al. Characteristics of the novel potassium-competitive acid blocker vonoprazan fumarate (TAK-438). Adv Ther. 2016;33:1140–57.
4. Shin JM, Inatomi N, Munson K, Strugatsky D, Tokhtaeva E, Vagin O. et al. Characterization of a novel potassium-competitive acid blocker of the gastric H,K-ATPase, 1-[5-(2-fluorophenyl)-1-(pyridin-3-ylsulfonyl)-1H-pyrrol-3-yl]-N-methylmethanamine monofumarate (TAK-438). J Pharmacol Exp Ther. 2011;339:412–20.
5. Sakurai Y, Nishimura A, Kennedy G, Hibberd M, Jenkins R, Okamoto H, et al. Safety, tolerability, pharmacokinetics, and pharmacodynamics of single rising TAK-438 (vonoprazan) doses in healthy male Japanese/non-Japanese subjects. Clin Transl Gastroenterol. 2015;6:e94.
6. Tanabe H, Ando K, Sato K, Ito T, Goto M, Sato T, et al. Efficacy of vonoprazan-based triple therapy for Helicobacter pylori eradication: A multicenter study and a review of the literature. Dig Dis Sci. 2017;62:3069–76.
7. Hoshikawa Y, Kawami N, Hoshino S, Tanabe T, Umezawa M, Kaise M, et al. Efficacy of on-demand therapy using 20-mg vonoprazan for non-erosive reflux disease. Esophagus. 2019;16:201–6.
8. Tanabe H, Yoshino K, Ando K, Nomura Y, Ohta K, Satoh K, et al. Vonoprazan-based triple therapy is non-inferior to susceptibility-guided proton pump inhibitor-based triple therapy for Helicobacter pylori eradication. Ann Clin Microbiol Antimicrob. 2018;17:29.
9. Yamasaki H, Kawaguchi N, Nonaka M, Takahashi J, Morohashi A, Hirabayashi H, et al. In vitro metabolism of TAK-438, vonoprazan fumarate, a novel potassium-competitive acid blocker. Xenobiotica 2017;47:1027–34.
10. Jung YS, Kim EH, Park CH. Systematic review with meta-analysis: the efficacy of vonoprazan-based triple therapy on Helicobacter pylori eradication. Aliment Pharmacol Ther. 2017;46:106–14.
11. Yoneyama T, Teshima K, Jinno F, Kondo T, Asahi S. A validated simultaneous quantification method for vonoprazan (TAK-438F) and its 4 metabolites in human plasma by the liquid chromatography-tandem mass spectrometry. J Chromatogr B Anal Technol Biomed Life Sci. 2016;1015–1016:42–9.
12. Hori Y, Imanishi A, Matsukawa J, Tsukimi Y, Nishida H, Arikawa Y. et al. 1-[5-(2-Fluorophenyl)-1-(pyridin-3-ylsulfonyl)-1H-pyrrol-3-yl]-N-methylmethanamine monofumarate (TAK-438), a novel and potent potassium-competitive acid blocker for the treatment of acid-related diseases. J Pharmacol Exp Ther. 2010;335:231–8.
13. Matsukawa J, Hori Y, Nishida H, Kajino M, Inatomi N. A comparative study on the modes of action of TAK-438, a novel potassium-competitive acid blocker, and lansoprazole in primary cultured rabbit gastric glands. Biochem Pharmacol. 2011;81:1145–51.
14. Jenkins H, Sakurai Y, Nishimura A, Okamoto H, Hibberd M, Jenkins R, et al. Randomised clinical trial: safety, tolerability, pharmacokinetics and pharmacodynamics of repeated doses of TAK-438 (vonoprazan), a novel potassium-competitive acid blocker, in healthy male subjects. Aliment Pharmacol Ther. 2015;41:636–48.
15. Suzuki T, Kagami T, Uotani T, Yamade M, Hamaya Y, Iwaizumi M, et al. Comparison of effect of an increased dosage of vonoprazan versus vonoprazan plus lafutidine on gastric acid inhibition and serum gastrin. Eur J Clin Pharmacol. 2018;74:45–52.
16. Xie Q, Chen Y, Liu F, Zhong Z, Zhao K, Ling Z, et al. Interspecies differences in metabolism of Deoxypodophyllotoxin in hepatic microsomes from human, monkey, rat, mouse and dog. Drug Metab Pharmacokinet. 2016;31:314–22.
17. Poulin P, Theil FP. Prediction of pharmacokinetics prior to in vivo studies. 1. Mechanism-based prediction of volume of distribution. J Pharm Sci. 2002;91:129–56.
18. Rodgers T, Leahy D, Rowland M. Physiologically based pharmacokinetic modeling 1: predicting the tissue distribution of moderate-to-strong bases. J Pharm Sci. 2005;94:1259–76.

Prediction of vonoprazan PK and PD using PBPK-PD model
WM Kong et al.

865

19. Chen Y, Zhao K, Liu F, Xie Q, Zhong Z, Miao M, et al. Prediction of Deoxypodophyllotoxin disposition in mouse, rat, monkey, and dog by physiologically based pharmacokinetic model and the extrapolation to human. Front Pharmacol. 2016;7:488.

20. Chen Y, Zhao K, Liu F, Li Y, Zhong Z, Hong S, et al. Predicting antitumor effect of Deoxypodophyllotoxin in NCI-H460 tumor-bearing mice on the basis of in vitro pharmacodynamics and a physiologically based pharmacokinetic-pharmacodynamic model. Drug Metab Dispos. 2018;46:897–907.

21. Shibata Y, Chiba M. The role of extrahepatic metabolism in the pharmacokinetics of the targeted covalent inhibitors afatinib, ibrutinib, and neratinib. Drug Metab Dispos. 2015;43:375–84.

22. Brown RP, Delp MD, Lindstedt SL, Rhomberg LR, Beliles RP. Physiological parameter values for physiologically based pharmacokinetic models. Toxicol Ind Health. 1997;13:407–84.

23. Hu ZY, Lu J, Zhao Y. A physiologically based pharmacokinetic model of alvespimycin in mice and extrapolation to rats and humans. Br J Pharmacol 2014;171:2778–89.

24. Li J, Guo HF, Liu C, Zhong Z, Liu L, Liu XD. Prediction of drug disposition in diabetic patients by means of a physiologically based pharmacokinetic model. Clin Pharmacokinet. 2015;54:179–93.

25. Yang J, Jamei M, Yeo KR, Tucker GT, Rostami-Hodjegan A. Prediction of intestinal first-pass drug metabolism. Curr Drug Metab. 2007;8:676–84.

26. Parrott N, Paquereau N, Coassolo P, Lave T. An evaluation of the utility of physiologically based models of pharmacokinetics in early drug discovery. J Pharm Sci. 2005;94:2327–43.

27. Guest EJ, Aarons L, Houston JB, Rostami-Hodjegan A, Galetin A. Critique of the two-fold measure of prediction success for ratios: application for the assessment of drug-drug interactions. Drug Metab Dispos. 2011;39:170–3.

28. Sakurai Y, Shiino M, Okamoto H, Nishimura A, Nakamura K, Hasegawa S. Pharmacokinetics and safety of triple therapy with vonoprazan, amoxicillin, and clarithromycin or metronidazole: a phase 1, open-label, randomized, crossover study. Adv Ther. 2016;33:1519–35.

29. Sakurai Y, Mori Y, Okamoto H, Nishimura A, Komura E, Araki T, et al. Acid-inhibitory effects of vonoprazan 20 mg compared with esomeprazole 20 mg or rabeprazole 10 mg in healthy adult male subjects-a randomised open-label crossover study. Aliment Pharmacol Ther. 2015;42:719–30.

30. Hori Y, Matsukawa J, Takeuchi T, Nishida H, Kajino M, Inatomi N. A study comparing the antisecretory effect of TAK-438, a novel potassium-competitive acid blocker, with lansoprazole in animals. J Pharmacol Exp Ther. 2011;337:797–804.

31. Qiao Y, Zhao J, Yue X, Zhang Y, Zhang R, Xu Y, et al. Study on pharmacokinetics and bioequivalence of vonoprazan pyroglutamate in rats by liquid chromatography with tandem mass spectrometry. J Chromatogr B Anal Technol Biomed Life Sci. 2017;1059:56–65.

32. Jenkins H, Jenkins R, Patat A. Effect of multiple oral doses of the potent CYP3A4 inhibitor clarithromycin on the pharmacokinetics of a single oral dose of vonoprazan: a phase I, open-label, sequential design study. Clin Drug Investig. 2017;37:311–6.

33. Dahlgren D, Roos C, Johansson P, Tannergren C, Lundqvist A, Langguth P, et al. The effects of three absorption-modifying critical excipients on the in vivo intestinal absorption of six model compounds in rats and dogs. Int J Pharm. 2018;547:158–68.

34. Willmann S, Thelen K, Becker C, Dressman JB, Lippert J. Mechanism-based prediction of particle size-dependent dissolution and absorption: cilostazol pharmacokinetics in dogs. Eur J Pharm Biopharm. 2010;76:83–94.

35. Guo H, Liu C, Li J, Zhang M, Hu M, Xu P, et al. A mechanistic physiologically based pharmacokinetic-enzyme turnover model involving both intestine and liver to predict CYP3A induction-mediated drug-drug interactions. J Pharm Sci. 2013;102:2819–36.

36. Kimura T, Higaki K. Gastrointestinal transit and drug absorption. Biol Pharm Bull. 2002;25:149–64.

37. Savic RM, Jonker DM, Kerbusch T, Karlsson MO. Implementation of a transit compartment model for describing drug absorption in pharmacokinetic studies. J Pharmacokinet Pharmacodyn. 2007;34:711–26.

38. Lin Z, Li M, Gehring R, Riviere JE. Development and application of a multiroute physiologically based pharmacokinetic model for oxytetracycline in dogs and humans. J Pharm Sci. 2015;104:233–43.

39. Kawai R, Lemaire M, Steimer JL, Bruelisauer A, Niederberger W, Rowland M. Physiologically based pharmacokinetic study on a cyclosporin derivative, SDZ IMM 125. J Pharmacokinet Biopharm. 1994;22:327–65.

40. DeSesso JM, Jacobson CF. Anatomical and physiological parameters affecting gastrointestinal absorption in humans and rats. Food Chem Toxicol. 2001;39:209–28.

41. Snipes. RL, Kriete. A. Quantitative investigation of the area and volume in different compartments of the intestine of 18 mammalian species. Z Fuer Saeugetierkunde. 1991;2:1860–3.

42. Eade MN, Ginn RW. The distribution of blood flow along the small intestine of the dog. Proc Soc Exp Biol Med. 1978;157:390–2.

43. Goodhead B. Distribution of blood flow in various selected areas of small and large intestine in the dog. Am J Physiol. 1969;217:835–7.